

$T_{1\rho}$ and $T_{2\rho}$ MRI in the evaluation of Parkinson's disease

I. Nestrasil · S. Michaeli · T. Liimatainen ·
C. E. Rydeen · C. M. Kotz · J. P. Nixon ·
T. Hanson · Paul J. Tuite

Received: 19 October 2009 / Revised: 21 December 2009 / Accepted: 22 December 2009 / Published online: 8 January 2010
© Springer-Verlag 2010

Abstract Prior work has shown that adiabatic $T_{1\rho}$ and $T_{2\rho}$ relaxation time constants may have sensitivity to cellular changes and the presence of iron, respectively, in Parkinson's disease (PD). Further understanding of these magnetic resonance imaging (MRI) methods and how they relate to measures of disease severity and progression in PD is needed. Using $T_{1\rho}$ and $T_{2\rho}$ on a 4T MRI scanner, we assessed the substantia nigra (SN) of nine non-demented moderately affected PD and ten gender- and age-matched control participants. When compared to controls, the SN of PD subjects had increased $T_{1\rho}$ and reduced $T_{2\rho}$. We also found a significant correlation between asymmetric motor features and asymmetry based on $T_{1\rho}$. This study provides additional validation of $T_{1\rho}$ and $T_{2\rho}$ as a means to separate PD from control subjects, and $T_{1\rho}$ may be a useful marker of asymmetry in PD.

Keywords Parkinson's disease ·
Magnetic resonance imaging · High-field MRI ·
Iron · Biomarker

Introduction

The pathogenesis of Parkinson's disease (PD) is influenced by genetic and/or environmental factors. Iron is increased in the substantia nigra (SN) in PD and is stored as ferritin or neuromelanin in neurons and glia [1, 2]. Release of iron could facilitate oxidative reactions, thereby leading to oxidative stress and subsequent neurodegeneration [3, 4]. It remains to be determined if iron deposition is affected by heavy metal environmental exposure, varying dietary metal intake, polymorphisms, or mutations in metal regulatory proteins or PD causative genes, or if it is a result of the

I. Nestrasil · P. J. Tuite (✉)
Department of Neurology, University of Minnesota,
MMC 295; 420 Delaware Street SE,
Minneapolis, MN 55455, USA
e-mail: tuite002@umn.edu

I. Nestrasil · S. Michaeli · T. Liimatainen
Department of Radiology, Center for Magnetic Resonance
Research, University of Minnesota, Minneapolis, USA
e-mail: nestr007@umn.edu

S. Michaeli
e-mail: shalom@cmrr.umn.edu

T. Liimatainen
e-mail: tliimata@cmrr.umn.edu

C. E. Rydeen · C. M. Kotz
Department of Neuroscience, University of Minnesota Medical
School, Minneapolis, USA
e-mail: rydee018@umn.edu

C. M. Kotz
e-mail: kotzx004@umn.edu

T. Hanson
Biostatistics Division, School of Public Health,
University of Minnesota, Minneapolis, USA
e-mail: hanson@biostat.umn.edu

C. M. Kotz
Department of Food Science and Nutrition,
University of Minnesota, Minneapolis, USA

J. P. Nixon
Minnesota Craniofacial Research Training Program,
School of Dentistry, University of Minnesota,
Minneapolis, USA
e-mail: nixon049@umn.edu

C. M. Kotz
Department of Veterans Affairs, Minneapolis, MN, USA

disease process and not necessarily causative [5]. Also, recent post-mortem work has demonstrated increased expression of a divalent metal transporter (DMT1/Nramp2/Slc11a2) isoform in the SN of PD brains, which suggests that this may enhance iron's entry into nigral neurons and hasten or facilitate PD pathogenesis [6].

Meanwhile, several research groups, including our own, have utilized iron sensitive magnetic resonance imaging (MRI) methods to separate individuals with PD from healthy controls [7–9]. Some techniques have also shown a relationship with the SN and lateralized motor scores but only with the more severely affected contralateral side [10, 11]. In a different study, Gorell et al. [9] presented a correlation of asymmetry of simple reaction time with asymmetries of SN iron-related contrasts generated with R_2^* and R_2' .

The present study was designed to: (1) replicate that neuronal-sensitive and iron-sensitive measures, $T_{1\rho}$ and $T_{2\rho}$, respectively, can separate PD from controls in a cross-sectional study; (2) determine if there is a correlation between clinical measures of PD and MRI relaxation times; and (3) evaluate if MRI methods could provide correlations with clinical asymmetry.

Methods

Patient and control subjects were recruited from the University of Minnesota Movement Disorders Clinic or through posted advertisements. Interested and eligible participants provided informed consent in this University of Minnesota Institutional Review Board-approved study. In addition to age- and gender-matched controls, subjects with a diagnosis of PD [12] who were taking and responding to antiparkinsonian medication were enrolled. All PD subjects were rated in their “on” motor state by the same neurologist (PT) using the complete Unified Parkinson's Disease Rating Scale (UPDRS), including the Hoehn and Yahr (H & Y) rating scale [13]. Individuals with dementia (as ascertained clinically and with a Mini-Mental State Examination score <24) and those unable to undergo a brain MRI were excluded from this study [14].

All scans were performed on an MRI system using a Varian Unity INOVA console (Varian Associates, CA) interfaced to a 90-cm bore 4T magnet (Oxford Magnet Technology, Oxford, UK). Transverse multislice images were obtained with a Rapid Acquisition with Relaxation Enhancement (RARE) sequence [repetition time (TR) = 4 s, echo train length = 8, echo spacing = 15 ms, echo time = 60 ms, seven slices, two averages]. Slices were positioned perpendicular to the longitudinal axis of the brainstem. The image of midbrain including the center of the red nucleus (RN) and mammillary body was selected

for the SN analysis [8]. $T_{1\rho}$ and $T_{2\rho}$ measurements were performed as described in prior work [15]. For $T_{1\rho}$ and $T_{2\rho}$, TurboFLASH imaging readout (four segments) was used [16]. $T_{1\rho}$ and $T_{2\rho}$ were assessed using 0.70 mm^2 in-plane resolution, FOV = 20 cm^2 , 256^2 matrix, and slice thickness = 3 mm. Thus, the digital pixel area is 0.49 mm^2 , and voxel volume is $1.5 \text{ }\mu\text{L}$. $T_{1\rho}$ and $T_{2\rho}$ measurements were performed using variable numbers (m) of hyperbolic secant adiabatic full passage (AFP) HS1 pulses using pulse time duration 0.006 s and calibrated to the peak power $\omega_1^{\text{max}} = 1.3 \text{ kHz}$ [17].

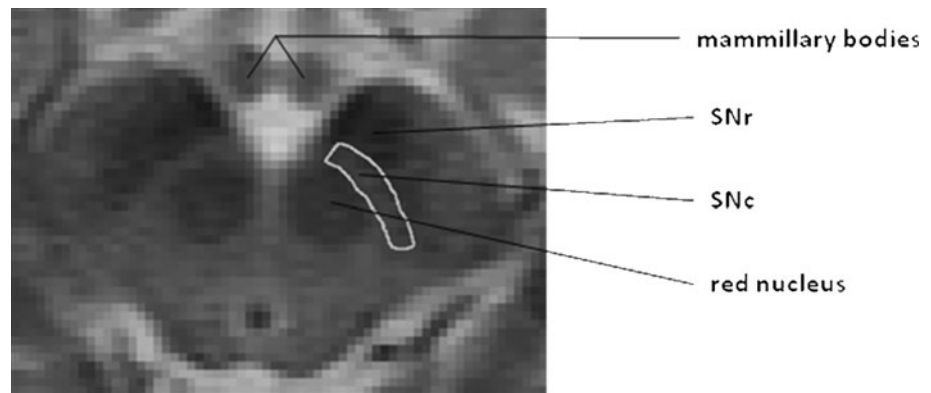
For $T_{2\rho}$ measurements, the AFP pulse train was placed after coherence excitation by an adiabatic half passage (AHP) pulse. Magnetization was returned back to the Z' axis using AHP pulse, and the TurboFLASH imaging readout was used. For $T_{1\rho}$ measurements, the AFP pulse train was placed prior to the coherence excitation by an AHP pulse.

Relaxation $T_{1\rho}$ and $T_{2\rho}$ maps were generated from pixel-by-pixel analysis using MATLAB software package (MATLAB 7.0, Mathworks, Natick, MA, USA). Region-of-interest (ROI) analyses were performed by one of the authors in a blinded manner. The process of segmenting acquired images of the SN into the pars reticularis (SNr) and pars compacta (SNc) is demanding as there is often interdigitation of tissue [10, 18]. From our images, a low signal intensity area which merges anteriorly into the cerebral peduncle corresponds to SNr and a relatively brighter crescent-shaped region located between SNr and RN may be SNc. In this study, we placed a ROI centrally in the hyperintense area of the region that we designate the SNc (Fig. 1). It was first placed in the RARE image and then copied to matching $T_{1\rho}$ and $T_{2\rho}$ maps. Statistical analyses were performed on the mean values of the relaxation time constants obtained from the ROIs. For each PD patient the degree of asymmetry of motor dysfunction [19] was determined according to the following formula:

$$\frac{\text{UPDRS right} - \text{UPDRS left}}{\text{UPDRS right} + \text{UPDRS left}} \times 2$$

UPDRS right and UPDRS left correspond to the sum of each side's UPDRS part III (motor UPDRS) ratings for rigidity, tremor, and bradykinesia (i.e., finger taps, hand grips, hand pronate/supinate, leg agility). The more negative scores imply more severe left-sided motor findings, and more positive scores correspond to more severe right-sided motor findings. Values of 0 represent symmetric motor impairment. The identical equation was used for calculation of $T_{1\rho}$ and $T_{2\rho}$ relaxation time constant asymmetries, respectively. A correlation between clinical and MRI asymmetry scores were calculated regarding a relation between the given SN and motor symptoms on the contralateral body side.

Fig. 1 RARE image showing boundaries of a representative example of the SNc in the midbrain. A region of interest (ROI) was placed centrally within the bright region that we designate the SNc



Statistical comparisons were based on results of the two-sided Student *t* test. In addition, a discriminatory ability of $T_{1\rho}$ and $T_{2\rho}$ was investigated using receiver operating characteristics (ROC) curves. As a measure of correlations between clinical and MRI findings, the Pearson product–moment correlation coefficient (*r*) was used. Only *p* values less than 0.05 were considered to indicate a significant difference.

Results

Nine patients with moderate PD and disease duration greater than 5 years [4 females (F) and 5 males (M)]; 59.0 ± 7.1 years [mean age \pm standard deviation (SD)] and ten age- and gender-matched healthy volunteers [5 F and 5 M; 59.3 ± 5.5 years (mean age \pm SD)] were included in this prospective study. The mean “ON state” UPDRS motor score was 31 ± 13 (mean age \pm SD), and the mean “on” state H&Y score was 2.5. Duration of PD after diagnosis was 7.67 ± 1.9 years (mean \pm SD). In Fig. 2, $T_{1\rho}$ versus $T_{2\rho}$ relaxation time constants of SNc are

plotted which shows a clear separation between the PD and control groups. ROC curves revealed good-to-excellent ability to differentiate between PD patients and healthy controls. The area under the ROC curve (AUC) for $T_{1\rho}$ is 0.989 (0.016), and for $T_{2\rho}$ the AUC is 0.956 (0.048). Both ($T_{1\rho}$, $T_{2\rho}$) together in a linear discriminant rule yields perfect classification for $AUC = 1.0$. Picking optimal cutoffs, the sensitivity of $T_{1\rho}$ was 1.00 with 95% (likelihood ratio) CI (0.81–1.00) and specificity 0.90 with 95% CI (0.63–0.99). The sensitivity of $T_{2\rho}$ was 0.89 (0.59–0.99) and specificity 1.00 (0.83–1.00). If both ($T_{1\rho}$, $T_{2\rho}$) are used together, the sensitivity and specificity reached 1.00 with 95% CI (0.81–1.00) for sensitivity and (0.83–1.00) for specificity. Figure 3 demonstrates a correlation between $T_{1\rho}$ -derived imaging asymmetry of the SNc and UPDRS III-based clinical asymmetry. No asymmetry was detected with $T_{2\rho}$. Significant differences for both $T_{1\rho}$ and $T_{2\rho}$ relaxation time constants between PD and control subjects are shown in Table 1. In the PD group, there were no significant correlations between the H&Y stage, duration of the disease, UPDRS scores (total

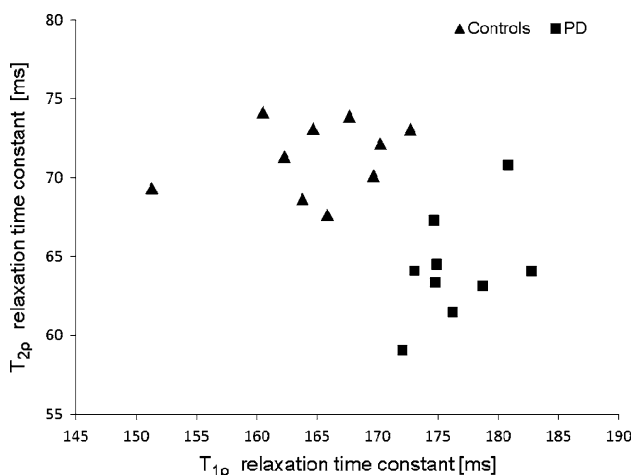


Fig. 2 Mean $T_{2\rho}$ versus $T_{1\rho}$ relaxation time constants of PD and control groups

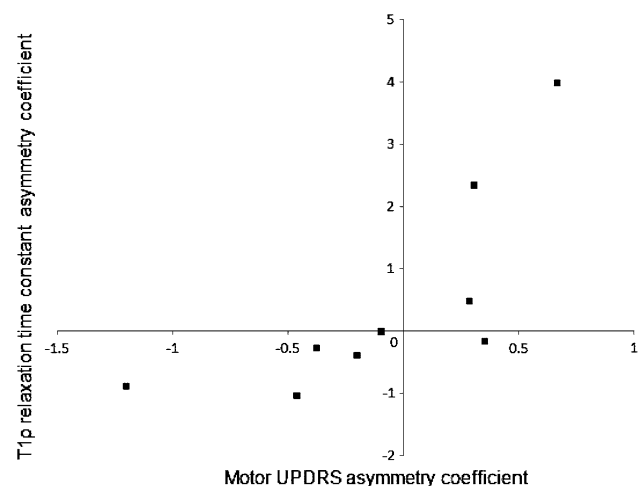


Fig. 3 Correlation between SNc $T_{1\rho}$ relaxation time constant asymmetry coefficient and motor UPDRS asymmetry coefficient ($r = 0.74$, $P = 0.02$)

Table 1 $T_{1\rho}$ and $T_{2\rho}$ relaxation time constants in PD and control subjects

	Relaxation time constant	
	$T_{1\rho}$ (MS)	$T_{2\rho}$ (MS)
PD	176.49 ± 6.46	64.19 ± 3.74
<i>P</i> values	<0.001	<0.001
Control	164.86 ± 6.78	71.35 ± 2.91

score or its subscores), and either contralateral $T_{1\rho}$ or $T_{2\rho}$ contrasts.

Discussion

This study showed that $T_{1\rho}$ and $T_{2\rho}$ of the “SNc” can distinguish patients with moderate PD from healthy age- and gender-matched controls, which further validates these MRI methods [8]. Compared to standard MRI techniques, utilization of adiabatic pulses at high magnetic fields enhances sensitivity of MRI to molecular motion in the local susceptibility gradients that arises from non-heme iron and tissue water–protein interactions. These methods have been shown to provide enhanced sensitivity to molecular dynamic processes over conventional T_1 and T_2 MRI methods as demonstrated in our prior work [8]. $T_{2\rho}$ provides information about diffusion and exchange of water protons in environments with different local susceptibilities, and as a result, the shortening of $T_{2\rho}$ is an indicator of iron content in tissue [8, 20]. Our results are in agreement with evidence of increased iron in the SN in PD [10, 11, 21]. Meanwhile, $T_{1\rho}$ contrast is considered to reflect differences in cell density by its specificity to water spin dynamics such as chemical exchange of protons between water associated with macromolecules and free water [8, 22–24]. The linkage of $T_{1\rho}$ and cell integrity is assumed from animal and human MRI studies [8, 23, 24]. Marked $T_{1\rho}$ increase in SNc as compared to controls was revealed in Pitx3-aphakia mice [23, 25]. In Pitx3 deficient mice SNc neurons vanish during development, which models loss of nigrostriatal neurons but not the gliosis in PD [23]. Human in vivo $T_{1\rho}$ -weighted MRI studies have shown changes in the hippocampus of Alzheimer’s patients [24] and in the SN of PD patients [8]. Both studies showed increased $T_{1\rho}$ in the diseased structures in patients, which suggests this measure is reflective of cellular density. Likewise, in this study we found increased $T_{1\rho}$ in the SN of PD versus controls. Although we evaluated a different cohort of PD subjects with longer duration of disease, we did not find a significant correlation between $T_{1\rho}$ or $T_{2\rho}$ and duration of disease, UPDRS scores, or stage of disease. This finding is congruent with previously published

cross-sectional MRI studies looking at iron in the SN [9–11] and with studies using transcranial sonography (TCS) of the SN [26]. As all PD subjects were scanned on medication, one cannot appreciate if there were medication effects on imaging findings, or if there would have been imaging correlates to “off” UPDRS scores. Presently it remains to be determined if these methods provide a measure of disease severity or a means for tracking progression.

Another aspect that this study focused on is the asymmetric nature of disease. With nuclear tracer imaging, the ability to demonstrate laterality of disease is well established [27–29]. In the present study we demonstrated a correlation with $T_{1\rho}$ but not $T_{2\rho}$ measures of the SN with an asymmetry ratio calculated from UPDRS motor scores. Moreover and similar to the Gorel et al. paper, no relationship was found between means of lateralized motor scores and both $T_{1\rho}$ or $T_{2\rho}$ measures of respective SNcs [9]. This finding might be due to the age range and severity of subjects evaluated in this study, which was different from Martin et al. where they evaluated untreated patients and from the Wallis et al. study where they included patients with a greater range of disease duration and all H&Y stages [10, 11].

In conclusion, we have demonstrated the ability of MRI methods to separate PD from controls. $T_{1\rho}$ may be a useful marker of asymmetry in mild-moderate PD.

Acknowledgments This study was supported by the University of Minnesota Academic Health Center, the University of Minnesota Undergraduate Research Opportunities Program, the University of Minnesota Medical Foundation, the National Institute of Dental & Craniofacial Research (T32DE007288), the National Institutes of Health (R01NS061866), and the Department of Veterans’ Affairs. We would like to acknowledge Heidi Vander Velden for her work as study coordinator and Dr. Michael A. Kuskowski (Minneapolis VA Medical Center, GRECC) for his assistance with the statistical analyses. T. Liimatainen was funded by the Instrumentarium Science Foundation, Orion Corporation Research Foundation, Finnish Cultural Foundation Northern Savo, and NIH grants P30 NS057091, P41 RR008079, R01NS061866 and R21NS059813.

Conflict of interest statement The authors report no conflict of interest.

References

1. Zecca L, Stroppolo A, Gatti A, Tampellini D, Toscani M, Gallorini M et al (2004) The role of iron and copper molecules in the neuronal vulnerability of locus ceruleus and substantia nigra during aging. *Proc Natl Acad Sci USA* 101(26):9483–9488
2. Faucheux BA, Martin ME, Beaumont C, Hauw JJ, Agid Y, Hirsch EC (2003) Neuromelanin associated redox-active iron is increased in the substantia nigra of patients with Parkinson’s disease. *J Neurochem* 86(5):1142–1148
3. Kaur D, Lee D, Ragapalan S, Andersen JK (2009) Glutathione depletion in immortalized midbrain-derived dopaminergic

- neurons results in increases in the labile iron pool: implications for Parkinson's disease. *Free Radic Biol Med* 46(5):593–598
4. Zecca L, Casella L, Albertini A, Bellei C, Zucca FA, Engelen M et al (2008) Neuromelanin can protect against iron-mediated oxidative damage in system modeling iron overload of brain aging and Parkinson's disease. *J Neurochem* 106(4):1866–1875
 5. Rhodes SL, Ritz B (2008) Genetics of iron regulation and the possible role of iron in Parkinson's disease. *Neurobiol Dis* 32(2):183–195
 6. Salazar J, Mena N, Hunot S, Prigent A, Alvarez-Fischer D, Arrendondo M et al (2008) Divalent metal transporter 1 (DMT1) contributes to neurodegeneration in animal models of Parkinson's disease. *Proc Natl Acad Sci USA* 105(47):18578–18583
 7. Hutchinson M, Raff U (2008) Detection of Parkinson's disease by MRI: Spin-lattice distribution imaging. *Mov Disord* 23(14):1991–1997
 8. Michaeli S, Oz G, Sorce DJ, Garwood M, Uğurbil K, Majestic S et al (2007) Assessment of brain iron and neuronal integrity in patients with Parkinson's disease using novel MRI contrasts. *Mov Disord* 22(3):334–340
 9. Gorell JM, Ordidge RJ, Brown GG, Deniau JC, Buderer NM, Helpem JA (1995) Increased iron-related MRI contrast in the substantia nigra in Parkinson's disease. *Neurology* 45(6):1138–1143
 10. Martin WR, Wieler M, Gee M (2008) Midbrain iron content in early Parkinson disease: a potential biomarker of disease status. *Neurology* 70(16):1411–1417
 11. Wallis LI, Paley MN, Graham JM, Grunewald RA, Wignall EL, Joy HM et al (2008) MRI assessment of basal ganglia iron deposition in Parkinson's disease. *J Magn Reson Imaging* 28(5):1061–1067
 12. Gelb D, Oliver E, Gilman S (1999) Diagnostic criteria for Parkinson disease. *Arch Neurol* 56(1):33–39
 13. Fahn S, Elton RL, members of the UPDRS Development Committee (1987) Unified Parkinson's disease rating scale. In: Fahn S, Marsden CD, Calne DB, Goldstein M (eds) *Recent developments in Parkinson's disease*. Macmillan Healthcare Information, Florham Park, pp 153–163
 14. Folstein M, Folstein S, McHugh PR (1975) "Mini-mental state". A practical method for grading the cognitive state of patients for the clinician. *J Psychiatr Res* 12(3):189–198
 15. Michaeli S, Grohn H, Grohn O, Sorce DJ, Kauppinen R, Springer CS Jr et al (2005) Exchange-influenced T2rho contrast in the human brain images measured with adiabatic radio frequency pulses. *Magn Reson Med* 53(4):823–829
 16. Haase Snapshot A, MRI FLASH (1990) Applications to T1, T2, and chemical-shift imaging. *Magn Reson Med* 13(1):77–89
 17. Silver MS, Joseph RI, Chen CN, Sank VJ, Hoult DI (1984) Selective population inversion in NMR. *Nature* 310(5979):681–683
 18. Damier P, Hirsch E, Agid Y, Graybiel A (1999) The substantia nigra of the human brain II. Patterns of loss of dopamine-containing neurons in Parkinson's disease. *Brain* 122:1437–1448
 19. Foster ER, Black KJ, Antenor-Dorsey JA, Perlmutter JS, Hershey T (2008) Motor asymmetry and substantia nigra volume are related to spatial delayed response performance in Parkinson's disease. *Brain Cogn* 67(1):1–10
 20. Haacke EM, Cheng NYC, House MJ, Liu Q, Neelavalli J, Ogg RJ et al (2005) Imaging iron stores in the brain using magnetic resonance imaging. *Magn Reson Imaging* 23(1):25
 21. Sofic E, Riederer P, Heinsen H, Beckmann H, Reynolds GP, Hebenstreit G et al (1988) Increased iron (III) and total iron content in postmortem substantia nigra of parkinsonian brain. *J Neural Transm* 74(3):199–205
 22. Grohn OH, Lukkarinen JA, Silvennoinen MJ, Pitkanen A, van Zijl PC, Kauppinen RA (1999) Quantitative magnetic resonance imaging assessment of cerebral ischemia in rat using on-resonance T(1) in the rotating frame. *Magn Reson Med* 42(2):268–276
 23. Michaeli S, Burns TC, Kudishevich E, Hanson T, Sorce DJ, Garwood M et al (2009) Detection of neuronal loss using T1rho MRI assessment of ¹H₂O spin dynamics in the aphakia mouse. *J Neurosci Methods* 177(1):160–167
 24. Borthakur A, Sochor M, Davatzikos C, Trojanowski JQ, Clark CM (2008) T1rho MRI of Alzheimer's disease. *Neuroimage* 41(4):1199–1205
 25. Michaeli S, Burns TC, Kudishevich E, Harel N, Hanson T, Sorce DJ et al (2009) Detection of neuronal loss using T1rho MRI assessment of ¹H₂O spin dynamics in the aphakia mouse. *J Neurosci Methods* 177(1):160–167
 26. Berg D, Merz B, Reiners K, Naumann M, Becker G (2005) Five-year follow-up study of hyperchogenicity of the substantia nigra in Parkinson's disease. *Mov Disord* 20(3):383–385
 27. Leenders KL, Salmon EP, Tyrrell P, Perani D, Brooks DJ, Sager H et al (1990) The nigrostriatal dopaminergic system assessed in vivo by positron emission tomography in healthy volunteer subjects and patients with Parkinson's disease. *Arch Neurol* 47(12):1290–1298
 28. Pirker W, Holler I, Gerschlager W, Asenbaum S, Zetting G, Brucke T (2003) Measuring the rate of progression of Parkinson's disease over a 5-year periods with beta-CIT SPECT. *Mov Disord* 18(11):1266–1272
 29. Benamer HT, Patterson J, Wyper DJ, Hadley DM, Macphee GJ, Grosset DG (2000) Correlation of Parkinson's disease severity and duration with 123I-FP-CIT SPECT striatal uptake. *Mov Disord* 15(4):692–698